Fluorogenic RNA aptamers to probe transcription initiation and co-transcriptional RNA folding by multi-subunit RNA polymerases

Yong-Heng Huang[1,†,#], Vilma Trapp[2,†], Oskari Puro[2], Janne J. Mäkinen[2], Mikko Metsä-Ketelä[2], Markus C. Wahl[1,3,*], Georgiy A. Belogurov[2,*]

[1] Freie Universität Berlin, Institute of Chemistry and Biochemistry, Laboratory of Structural Biochemistry, Takustr. 6, D-14195 Berlin, Germany

[2] University of Turku, Department of Life Technologies, FIN-20014 Turku, Finland

[3] Helmholtz-Zentrum Berlin für Materialien und Energie, Macromolecular Crystallography, Albert-Einstein-Str. 15, D-12489 Berlin, Germany

[†] Shared first authors; these authors contributed equally to this work.

[#] Present address: GenScript Corporation, Protein Production Department, No. 28 Yongxi Road, 211100 Nanjing, China; hheng888@163.com

[*] Correspondence to: markus.wahl@fu-berlin.de; gebelo@utu.fi

Published article URL and doi:

https://www.sciencedirect.com/science/chapter/bookseries/abs/pii/S0076687922002488

https://doi.org/10.1016/bs.mie.2022.07.010

Contents

Abstract

Transcription is the first and most highly regulated step in gene expression. Experimental techniques for monitoring transcription are, thus, important for studying gene expression and gene regulation as well as for translational research and drug development. Fluorescence methods are often superior to other techniques for real-time monitoring of biochemical processes. Green fluorescent proteins have long served as valuable tools for studying the process of translation. Here we present two methods that utilize fluorescent light-up RNA aptamers (FLAPs), the RNA mimics of green fluorescent proteins, to monitoring transcription and co-transcriptional RNA folding. FLAPs adopt defined three-dimensional folds that bind low molecular weight compounds called fluorogens with concomitant increase in fluorescence by many folds. FLAPs provide a strong fluorescence signal with low background that allows monitoring of transcription in real time *in vitro* and *in vivo*. However, it takes several seconds for RNA polymerase to synthesize FLAPs and the subsequent folding of the fluorogen-binding platform takes additional seconds or minutes. Here we show that Broccoli-FLAP is well suited for monitoring the rate of transcription initiation in a multi-round setup that mitigates the slow rate of the FLAP maturation. Furthermore, we demonstrate that a relatively slow and inefficient folding of iSpinach-FLAP can be taken advantage of for monitoring the action of RNA folding chaperones.

1. Introduction

Transcription is the synthesis of RNA using DNA as a template. It is the first and most regulated step in gene expression. Transcription of cellular genomes is catalyzed by multi-subunit RNA polymerases (RNAPs) of the two-barrel structural class (Iyer et al., 2003; Werner & Grohmann, 2011), whereas transcription of mitochondrial genomes is catalyzed by single-subunit RNAPs of the right-hand structural class (Cermakian et al., 1997). The ability to monitor transcription *in vitro* and *in vivo* is essential for studying the functioning of life forms from viruses to humans, translational research, and drug development. The bacterial RNAP, a minimally five subunit $\alpha_2\beta\beta'\omega$ complex, is the simplest multi-subunit RNAP and only requires a single additional subunit called the σ factor for the initiation of transcription at a promoter. In this chapter we describe the use of fluorogenic RNA aptamers to study transcription initiation and co-transcriptional RNA folding catalyzed by bacterial RNAP and associated transcription factors *in vitro*.

Traditionally transcription has been monitored by analyzing RNA products by gel electrophoresis. These methods are the preferred techniques in transcription research as they directly reveal the products of transcription reactions and often allow monitoring of transcription with single nucleotide precision (see e.g., (Artsimovitch et al., 2003)). However, these techniques are very laborious, low throughput, and are difficult to automate. The

significant increase in price of the ^{32}P-labeled nucleoside triphosphates (NTPs) recently introduced an additional burden for the application of such approaches. In studies of transcription elongation (Komissarova et al., 2003), end-labeling of RNA primers with fluorophores is an adequate substitute for labeling with ^{32}P (Prajapati et al., 2019). The same is not true for the studies of transcription initiation, where two individual nucleotides are joined together in the RNAP active site and the employment of NTPs with bulky modifications such as fluorophores is highly undesirable.

Many RNAs adopt complex and dynamic 3D structures to exert their cellular functions (reviewed in (Ganser et al., 2019)). It has long been noted that RNAs fold co-transcriptionally and that co-transcriptional RNA folding feeds back on transcription and profoundly influences nascent RNA processing and co-transcriptional RNA-protein complex assembly (reviewed in (Schärfen & Neugebauer, 2021; Zhang & Landick, 2016)). Important parameters influencing co-transcriptional RNA folding are the inherent directionality of the transcription process, determining in which order interacting regions of the transcript are produced, and the transcription kinetics, in particular RNAP pausing at particular sites. However, transcription complexes, specifically portions of RNAP and associated transcription factors, may also strongly influence co-transcriptional RNA folding by providing transient binding platforms for nascent RNA regions and thereby acting essentially as co-transcriptional RNA chaperones (reviewed in (Said & Wahl, 2021; Zhang & Landick, 2016)). Elaborate biochemical and biophysical methods have been developed to monitor co-transcriptional RNA folding in real time *in vitro* and *in vivo*, including, e.g., chemical probing in combination with RNA sequencing or single-molecule spectroscopy-based techniques (reviewed in (Dangkulwanich et al., 2014; Ganser et al., 2019; Leamy et al., 2016)). These methods can also inform on the impact of RNAP regions and RNAP-associated factors on nascent RNA folding, and the results can be further integrated using computational approaches (Yu et al., 2021). However, these methodologies require elaborate equipment, special expertise and/or are experimentally or computationally comparatively demanding.

In this chapter we present two transcription assays in which the transcribed RNA encodes an aptamer that binds a low molecular weight fluorogenic compound (fluorogen) with high affinity and specificity. The fluorogen is virtually non-fluorescent when free in the aqueous solution. Binding of the fluorogen to the aptamer significantly (50-100-fold) increases the fluorescence of the fluorogen, thereby providing an easy means to monitor the accumulation of the product RNA in real time. The aptamer-fluorogen combinations are often referred to as fluorescent light-up aptamers or FLAPs (Neubacher & Hennig, 2019). The two assays presented here utilize iSpinach (Autour et al., 2016; Fernandez-Millan et al., 2017) and Broccoli (Filonov et al., 2014) aptamers. Both aptamers are RNA mimics of the green fluorescent protein because they enhance the fluorescence of compounds that resemble the chromophore of the green fluorescent protein. An extensive collection of FLAPs that

fluorescence at markedly different wavelengths has been developed in recent years (reviewed in (Neubacher & Hennig, 2019)).

iSpinach and Broccoli (tRNA embedded) FLAPs are 70-120 nt long and are thus relatively low-resolution reporters: it takes several seconds for RNAP to synthesize them, and it takes additional time (seconds or minutes) for aptamers to fold and bind fluorogens (Huang et al., 2020). Accordingly, carefully adjusted experimental conditions and a detailed understanding of the processes taking place in the assay mixture are needed to extract quantitative data from the FLAP-based assays.

The first assay that we describe in this chapter is a multi-round assay based on Broccoli-FLAP and involving the entire transcription cycle. Despite the overall complexity of the processes taking place in the assay mixture, the resulting fluorescence time traces have only two distinct phases: a lag phase that incorporates all events leading to the generation of the fluorescent signal, and a linear phase that exclusively reports the rate of transcription initiation. The assay relies on manual mixing of the reactants, is performed in a conventional fluorometer using an ultra-micro cuvette and can be potentially adapted to a plate reader format.

The second assay in this chapter is a single-round assay for monitoring co-transcriptional RNA folding and is based on iSpinach-FLAP. The assay is performed with a pre-formed transcription elongation complex (EC) to speed up the FLAP synthesis thereby maximizing the contribution of the FLAP folding kinetics to the rate of the fluorescence increase. However, the most important observation is that higher amplitudes of the fluorescence increase are observed in the presence of RNA folding chaperones (Huang et al., 2020). Apparently, only a fraction of the iSpinach folds into a FLAP when synthesized by RNAP alone providing a headroom for the assessment of the activity of RNA folding chaperones. The assay is performed in a dedicated rapid mixing device such as a stopped-flow instrument.

2. Multi-round Broccoli-FLAP assay for monitoring transcription initiation

The assay involves a complete transcription cycle: the σ factor-dependent initiation at the promoter, transcription elongation using the double-stranded DNA as a template and transcription termination at a bacterial RNA hairpin-dependent terminator (Fig. 1). The assay is multi-round: following the termination of transcription, RNAP rebinds the σ factor and repeats the entire cycle. Repeating rounds of transcription produce increasing amounts of the RNA aptamer that binds and “lights up" the fluorogen, resulting in the time-dependent increase in fluorescence. The slope of the fluorescence increase time traces reports the rate of transcription initiation. The assay is suitable for assessing the strength of bacterial promoters, initiation competence of wild-type and altered RNAPs and σ factors, as well as for

monitoring the effects of additives, such as proteins of interest (POI) or small molecular compounds of interest (COI) on the transcription initiation.

2.1 Equipment

- Spectrofluorometer, LS-55 (Perkin Elmer) with thermostated cuvette holder
- Circulator bath for temperature control of the cuvette
- Ultra-micro cuvette Hellma 105.251-QS
- Thermomixer or thermoblock for 1.5 ml microcentrifuge tubes
- Low protein binding microcentrifuge tubes
- DNAse-RNAse free aerosol resistant tips

Alternatives:

- Sub-micro or ultra-micro cuvettes: Starna 16.50-F/Q/10, Starna 16.100-F/Q/10, Hellma 105.250-QS, Starna 16.160-F/Q/10.
- Coarse sand bath can be used instead of a thermoblock/thermomixer

2.2 Buffers and reagents

- Milli-Q water treated with diethyl pyrocarbonate (DEPC).
- Enzyme Storage Buffer (10 mM Tris-HCl pH 7.5, 50% glycerol, 100 mM NaCl, 0.1 mM EDTA, 0.1 mM DTT).
- 10 x concentrate of Transcription Buffer (400 mM HEPES-KOH pH 7.5, 800 mM KCl, 50 mM $MgCl_2$, 50% glycerol, 1 mM EDTA, and 1 mM DTT).
- DFHBI-1T, 1 mM stock in DMSO. DFHBI-1T= (5Z)-5-[(3,5-Difluoro-4-hydroxyphenyl)methylene]-3,5-dihydro-2-methyl-3-(2,2,2-trifluoroethyl) -4H-imidazol-4-one.
- Ultra-pure nucleoside triphosphates (NTPs): ATP, CTP, GTP, UTP from Jena Bioscience, (Jena, Germany).

Alternatives:

- Ultra-pure NTPs can also be purchased from Thermo Fisher Scientific (Waltham, MA, United States) and Cytiva (Marlborough, MA, United States).

Critical:

- All reagents used should be RNase-free grade or treated with DEPC. Solutions containing DFHBI-1T should be protected from exposure to light. DTT is added freshly from a frozen 1 M stock immediately before use.

2.3 Proteins and nucleic acids

- In-house purified (Svetlov & Artsimovitch, 2015) *E. coli* RNAP, 50 μM stock in Storage Buffer

- In-house purified (Krupp et al., 2019) *E. coli* σ70 initiation factor, 200 μM stock in Storage Buffer
- *Saccharomyces cerevisiae* inorganic pyrophosphatase, in house purified (Heikinheimo et al., 1996) or commercial, ~10 μM stock in Storage Buffer.
- pOP004 plasmid, 500 nM stock purified from 500 ml of the overnight *E. coli* culture using NucleoBond Xtra Maxi Plus EF kit (Macherey-nagel, Düren, Germany).

Alternatives:

- Linear DNA templates generated by PCR can be used instead of circular plasmid DNA templates.

2.4 Procedure

1. Turn on the spectrofluorometer including the light source.
2. Turn on the temperature control of the cuvette compartment (circulator water bath or Peltier based system if equipped), set the temperature to 37 °C.
3. Place the ultra-micro cuvette into the thermostated cuvette holder.
4. Prepare 40 μl holoenzyme mix containing excess of σ70 (Table 1). Incubate at 30 °C for 20 minutes, store at -20 °C. POI (in Storage Buffer) may be added to the holoenzyme mix and the volume of the Storage Buffer reduced accordingly.

Table 1. Holoenzyme mix for five time traces (see notes 1-2).

Volume	Component	Concentration	
		in the mix	in the assay
24 μl	1× Storage Buffer	1×	0.1×
8 μl	RNAP (50 μM stock in Storage Buffer)	10 μM	1 μM
8 μl	σ factor (200 μM stock in Storage Buffer)	40 μM	4 μM

5. Prepare 160 μl of the DNA template mix (Table 2). Place and store on ice.

Table 2. DNA mix for five time traces (see notes 1 and 3).

Volume	Component	Concentration	
		in the mix	in the assay
116 μl	Milli-Q water		
20 μl	10× Transcription Buffer	1.25×	1×
4 μl	DFHBI-1T (1 mM stock)	25 μM	10 μM
4 μl	Pyrophosphatase (10 μM stock)	0.25 μM	0.1 μM
16 μl	pOP004 plasmid (500 nM stock)	50 nM	20 nM

6. Prepare 200 µl of NTP mix (Table 3). Place and store on ice. COI may be added to the NTP mix and the volume of the Milli-Q water reduced accordingly.

Table 3. NTP mix for five time traces (see notes 1 and 4).

Volume	Component	Concentration	
		in the mix	in the assay
164 µl	Milli-Q water		
20 µl	10 x Transcription Buffer	1×	1×
4 µl	ATP (100 mM)	2 mM	1 mM
4 µl	CTP (100 mM)	2 mM	1 mM
4 µl	GTP (100 mM)	2 mM	1 mM
4 µl	UTP (100 mM)	2 mM	1 mM

7. Start the spectrofluorometer control software, set the measurements as follows:
   - Mode: Time drive (continuous measurement at one wavelength).
   - Time: 600 seconds
   - Time intervals: 1 sec
   - Excitation wavelength: 472 nm
   - Emission wavelength: 507 nm
   - Excitation and emission slit width: 10 nm
   - Immediate start - check
   - Auto increment file names - check
8. Pipette 28 µl of DNA mix (stored on ice) into a microcentrifuge tube, add 7 µl of Holoenzyme mix (stored at -20 °C), place the tube to 37 °C thermomixer.
9. Pipette 40 µl of NTPs mix into a microcentrifuge tube, place the tube to 37 °C thermomixer for 2 min.
10. Withdraw 35 µl of prewarmed NTPs mix into a pipette tip, start timer, pipette the prewarmed NTPs mix into the tube with 35 µl of prewarmed DNA-holoenzyme mix, mix gently by pipetting up and down three times.
11. Transfer 55 µl of the DNA-holoenzyme-NTPs mix into the cuvette (prewarmed in the thermostated spectrofluorometer holder), place the cuvette back into the spectrofluorometer.
12. Start recording the fluorescence time trace when timer displays 20 s (see note 5). Stop recording after 10 min (see note 6).
13. Withdraw the reaction mixture from the cuvette as soon as possible after stopping the recording. Rinse the cuvette with water, 0.1 M HCl, followed by three times with water.

14. Return to step 8 to record the next time trace.
15. After finishing recording all time traces. Export the fluorescence time traces into the spreadsheet software (Excel, Origin). Add 20 s to the time-base (see note 7) and further analyze as described below.

2.5 The expected outcome.

Fluorescence time traces will feature a lag phase, until transcription yields a complete DFHBI-1T binding Broccoli-FLAP platform. Subsequently, the fluorescence signal will increase near linearly if sufficient NTPs are provided (Fig. 2AB). Some templates output perfectly linear time traces at high NTPs (pOP005, Fig. 2A), whereas on other templates transcription rate decreases slightly as transcription proceeds (pOP004, Fig. 2B). The slope of the near linear phase can be adjusted by manipulating the DNA template concentration (Fig. 2C). The presence of POI or COI may increase or decrease the duration of the lag phase (if the additive affects the elongation rate or folding of Broccoli-FLAP) and increase or decrease the slope of the near linear phase (if the additive affects the initiation rate). POI and COI may also turn linear traces into curved traces or the other way around. Both circular and linear templates can be used when the Broccoli gene is placed under control of a strong promoter and followed by an efficient terminator. Linear templates are preferred if the Broccoli gene is placed under control of a weak promoter, and if POI or COI with antitermination activities are being investigated.

2.6 Quantification and statistical analysis

Mixing the reactants initiates the pre-steady state phase where RNAP holoenzymes initiate transcription for the first time (Fig. 3A). After pioneering RNAPs escape promoters and continue elongating the transcript, the second set of holoenzymes binds to the promoter and initiates transcription followed by the third set and so on. Within 1-2 min, pioneering RNAPs complete the synthesis of the Broccoli-FLAP (~0.7 kb between the promoter and the 3' end of the FLAP) and get recycled at the intrinsic terminator. In graphical terms, the pre-steady state phase corresponds to the lag phase where practically no change in fluorescence is observed.

Within 1-2 min (for ~1 kb transcription unit and *E. coli* RNAP at 37 °C) a steady state is established where a fraction of RNAPs are engaged in transcript elongation, whereas the rest initiate transcription as soon as promoters dispatch the previous set of RNAPs into elongation. This steady-state phase corresponds to a linear or near linear increase in fluorescence with the slope corresponding to the initiation rate (Fig. 3BCD). In experiments in which the steady-state phase is perfectly linear, a linear fit with a time offset can be used to determine the slope (Fig. 3C):

If ($x<t_o$) $F(t)=F_o$ else $F(t)=F_o+k*(t-t_o)$.

In which F(t) is the fluorescence at time t, F_o is the initial fluorescence, t_o is a time offset, k is the slope. The initiation rate (slope) is initially determined in "fluorescence units per second"

but can be further converted to "initiation events per second per promoter" by calibrating the assay with a known amount of FLAP-RNA (see below).

The time offset value approximately corresponds to the duration of the lag phase and includes (*i*) the time it takes for RNAP to transcribe from the promoter to the 3′ end of the FLAP, and (*ii*) the time it takes for FLAP to fold and bind the fluorogen. Transcription templates with the 3′ end of the FLAP positioned 0.2 and 0.7 kb downstream of the promoter display a similar lag phase when assayed at 5 mM total Mg^{2+} (Fig. 3CD), suggesting that the FLAP maturation step significantly contributes to the duration of the lag phase under such conditions. Accordingly, we advise against inferring the transcription elongation rate from the duration of the lag phase when using relatively short templates as described in this protocol. That said, in qualitative terms, an increase in the duration of the lag phase, if observed, most likely reflects the decrease in the rate of transcription elongation.

More often than not the steady state phase of the multi-round transcription assay is not perfectly linear even at high [NTPs] (Fig. 3D). Processes such as poisoning of the transcription template by stalled RNAPs, changes in the template supercoiling and gradual inactivation of RNAP may possibly be responsible for the gradual decrease of the transcription initiation rate as transcription proceeds. The near linear fluorescence time traces are often adequately described by a single exponential function with the time offset (Fig. 3D):

If ($x<t_o$) $F(t)=F_o$ else $F(t)=F_o+A*(1-\exp(-k*(t-t_o)))$.

In which F(t) is the fluorescence at time t, F_o is the initial fluorescence, t_o is a time offset, A is a pre-exponent parameter, and k is an exponent parameter.

Noteworthy, the single exponential function unlikely reflects the underlying kinetic mechanism of the process (see notes 8 and 9) and is used solely as an empirical function to estimate the initiation rate. The product (multiplication, A*k) of the exponent and the pre-exponent corresponds to the initiation rate in fluorescence units per second. The time offset approximately corresponds to the duration of the lag phase and should be interpreted and handled as described above for the time offset of a linear fit.

The initiation rate in "fluorescence units per second" can be further converted to "initiation events per second per promoter" by calibrating the assay with a known amount of the FLAP-RNA. The FLAP-RNA is first produced by *in vitro* transcription using a linear DNA fragment as a template and purified. Known amounts of the FLAP-RNA are then added to the assay mixture instead of NTPs and the step-increase in fluorescence is measured. Dividing the step-increase in fluorescence by the calculated molar concentration of FLAP-RNA generates a FU-to-nM coefficient (Fluorescence Units to nM of FLAP-RNA). The initiation rate in "fluorescence units per second" is divided by FU-to-nM and by the promoter concentration in nM to estimate the rate in "initiation events per second per promoter".

For statistical analysis, three or more fluorescence time traces are fitted independently using either linear or single exponential function with a time offset. The inferred parameters are then analyzed to determine the average values and SDs. In cases where the time traces have complex shapes and are not readily amenable to fitting, three or more fluorescence time traces are averaged and plotted together with SDs for each timepoint. A graphic comparison of the time traces obtained in the presence and absence of the additives is then used to make qualitative conclusions about the effects of the additives.

2.6 Notes

1. The reasoning behind the formulation of the solutions is as follows. The holoenzyme is prepared as a separate mix so it can be stored at -20 °C and an equally fresh aliquot is used for each measurement. Shortly prior to the start of the transcription reaction, the aliquots of the holoenzyme mix and the DNA mix are mixed in 1:4 ratio to arrive at an aliquot of the holoenzyme-DNA mix. The transcription reaction is then initiated by mixing equal volumes of the holoenzyme-DNA mix and the NTP mix. Starting the reaction by mixing equal volumes of two solutions results in optimal mixing and pipetting convenience (the mixture can be gently pipetted back and forth without changing the pipette setting and without risking introducing air bubbles). The volumes of the mixtures suffice for the recording of five time traces with some excess volume allocated for pipetting convenience (i.e., it is seldom possible to withdraw 20 µl from a tube containing 20 µl of a solution). The final composition of the transcription mixture is presented in Table 4.

Table 4. The composition of the transcription reaction mixture (see notes 1-4).

Component	Final concentration
HEPES-KOH pH 7.5	40 mM
Glycerol	10%
DMSO	1%
KCl	80 mM
NaCl	10 mM
$MgCl_2$	5 mM
Tris-HCl pH 7.5	1 mM
ATP, CTP, GTP, UTP	1 mM each
EDTA	0.11 mM
DTT	0.11 mM
DFHBI-1T	10 µM
RNAP	1 µM
σ factor	4 µM

Pyrophosphatase	0.1 μM
DNA template	20 nM

2. 1-2 μM RNAP ensures that RNAP is present in excess over the 20-40 nM of promoter driving the ~1 kb transcription unit. Assuming a promoter activity of 0.1 initiations per second and transcription elongation rate of 10 nt/s (a lower bound for *E. coli* RNAP at 25-37 °C), a RNAP density of one per 100 bp is expected. This translates to about ten RNAP molecules being engaged in transcription elongation of a ~1 kb transcription unit. 20-40 nM of DNA template are then anticipated to sequester 200-400 nM of RNAP in the elongation phase of transcription.

3. 20-80 nM of the DNA template is a usable range in most cases.

4. 1 mM of each NTP and 5 mM Mg^{2+} total (= free Mg^{2+} ~1 mM) strike a balance between providing enough Mg^{2+} complexed NTPs for the measurement timeframe and minimizing the precipitation of transcription byproducts at high Mg^{2+} concentration. 0.5-1 mM NTPs, 5-10 mM Mg^{2+} are usable ranges in most cases. 0.1-0.25 mM NTPs result in significant depletion of the NTP pool during the measurement timeframe and can be used for specific purposes such as evaluating the effects of the additives (COI or POI) on the substrate affinity.

5. If mixing the holoenzyme-DNA and NTPs solutions and the transfer of the resulting mix to the cuvette takes longer than 20 s, the recording can be initiated at 30 s.

6. Longer measurement times can result in the precipitate of magnesium pyrophosphate and phosphate in the cuvette. Shorter measurement times are recommended for faster reactions and longer measurement times may be possible for slower reactions. It is advisable not to exceed the time it takes for 1 mM of pyrophosphate to form in the reaction mixture which approximately corresponds to the complete consumption of 250 μM of each NTP.

7. If the recording was started at 30 s, add 30 s to the time-base rather than 20 s.

8. For time traces where the depletion of NTPs is the main reason for the decrease of the transcription initiation rate with time (e.g., time traces measured at 0.1 mM NTPs in Fig. 2AB), the integral form of the Michaelis equation with a time offset is likely the most appropriate function describing the underlying mechanism of the process. While the integral of the Michaelis equation can be used to fit time traces of the fluorescence increase, doing so requires sophisticated fitting software capable of the numerical integration of a piecewise function with a time offset as a free parameter.

9. All types of fits described in this section ignore the curvature of the transition between the lag phase and the near linear increase in fluorescence (Fig. 3B). We suggest that the asynchronous arrival of the pioneering RNAPs to the 3′ end of the Broccoli gene is likely the

main factor determining the curvature of the interphase segment. The emergence of the fluorescence signal is also a sequential reaction consisting of Broccoli-FLAP production followed by the Broccoli-FLAP folding and binding of the fluorogen. The sequential nature of the process may additionally contribute to the curvature of the interphase segment. Although clearly visible in most fluorescence time traces, the interphase segment can be disregarded when fitting the entire 5-10 min time trace: the transition is represented by a relatively small number of time points and has little impact on the fit statistics.

3. Single-round iSpinach-FLAP assay for monitoring co-transcriptional RNA folding.

Here we present a protocol that can be used to investigate the effects of RNAP variants, RNAP-associated transcription factors or other cues on co-transcriptional RNA folding. The co-transcriptional RNA folding assay monitors the production of iSpinach-FLAP, whose native fold comprises a complex structure with a central G-quadruplex element assembled from distal regions. Properly folded iSpinach presents a binding platform that will quickly accommodate a low molecular weight fluorogen, DFHBI, giving rise to a fluorescence signal.

The assay is performed as follows. First, a stable transcription EC is formed by the σ factor-dependent initiation from a bacterial promoter in the presence of a subset of NTPs. In this preparatory step, RNAP initiates from a dinucleotide primer (ApU), transcribes 33 positions, and stops when encountering a position that requires an omitted NTP substrate (UTP). The transcription is performed at low concentration of NTPs to prevent read-through the stop position (where the omitted NTP is required) due to misincorporation. A pre-formed EC is used to ensure a rapid and synchronous start of transcription. Second, the pre-formed EC is mixed with a chase solution that contains all four NTPs at high concentration to start transcription of the bulk of the ~100-nt long FLAP-RNA. Following the transcription of the FLAP, RNAP falls off the linear DNA template. The transcription inhibitor rifampicin is added to the chase mix to prevent re-initiation of transcription, thereby ensuring that only a single round of transcription takes place. Transcribed FLAP-RNA binds the fluorogen with concomitant increase in fluorescence that is continuously monitored in the stopped-flow instrument.

We have shown recently that RNAP-associated RNA chaperones significantly increase the rate and the amplitude of the fluorescence increase during transcription of iSpinach by *E. coli* RNAP (Huang et al., 2020). These observations suggest that only a fraction of iSpinach aptamer folds into a FLAP correctly when emerging from the RNAP, and a larger fraction folds correctly if assisted by RNA folding chaperones near the RNA exit channel. The iSpinach system is therefore uniquely suitable for monitoring the co-transcriptional RNA folding.

3.1 Equipment

- SX20 Stopped-Flow Fluorescence Spectrophotometer, Applied Photophysics
- Circulator water bath for temperature control
- Thermomixer or thermoblock for 1.5 ml microcentrifuge tubes
- PCR cycler (for DNA template manufacture)
- Low protein binding microcentrifuge tubes
- DNAse-RNAse free aerosol resistant tips

Alternatives:

- Stopped-flow fluorescence spectrophotometer from KinTek Corporation (Snow Shoe, PA, USA) or BioLogic (Seyssinet-Pariset, France).

3.2 Buffers and reagents

- Milli-Q water treated with diethyl pyrocarbonate (DEPC).
- Enzyme Storage Buffer (10 mM Tris-HCl pH 7.5, 50% glycerol, 100 mM NaCl, 0.1 mM EDTA, 0.1 mM DTT).
- 10 x concentrate of Transcription Buffer (200 mM HEPES-NaOH pH 7.5, 1M KCl, 50 mM $MgCl_2$, 50 mM DTT).
- DFHBI, 2 mM stock in DMSO. DFHBI = (5Z)-5-[(3,5-Difluoro-4-hydroxyphenyl)methylene]-3,5-dihydro-2,3-dimethyl-4H-imidazol-4-one.
- 10 mM rifampicin solution in methanol.
- ApU RNA dinucleotide, 1 mM stock, Jena Bioscience (Jena, Germany).
- Ultra-pure nucleoside triphosphates (NTPs): ATP, CTP, GTP, UTP from Jena Bioscience, (Jena, Germany).

Alternatives:

- Ultra-pure NTPs can also be purchased from Thermo Fisher Scientific (Waltham, MA, United States) and Cytiva (Marlborough, MA, United States).

Critical:

- All reagents used should be RNase-free grade or treated with DEPC. Solutions containing DFHBI and/or rifampicin should be protected from exposure to light. DTT is added freshly from a frozen 1 M stock immediately before use.

3.3 Proteins and nucleic acids

- In-house purified (Svetlov & Artsimovitch, 2015) *E. coli* RNAP, 100 μM stock in Storage Suffer
- In-house purified (Krupp et al., 2019) *E. coli* σ70 initiation factor, 100-400 μM stock in Storage Buffer

- In-house purified (Huang et al., 2020) RNA folding chaperones, e.g. *E. coli* NusA elongation factor, 100-200 μM stock in Storage Buffer
- Linear DNA template (2 μM stock) generated by large-scale PCR (40 x 50 μl, 2 ml total volume) using pISPINACH plasmid as a template and purified using PCR Clean-up Kit (Macherey-nagel, Düren, Germany).

Alternatives:

- Linear DNA template can be purified from PCR reaction by anion exchange chromatography using Mono Q 5/50 GL column (GE Healthcare) followed by precipitation with isopropanol, wash with 70% ethanol and resuspension in 50-100 μl of milliQ water.

3.4 Procedure

1. Turn on the stopped flow instrument including the light source.
2. Turn on the water bath circulator, set the temperature to 32 °C.
3. Install a 495 nm long-pass filter between the photomultiplier tube and the mixing cell. **Caution! Ensure that no voltage is applied to photomultiplier tube when performing this operation. Refer to the instrument manual for details.**
4. Adjust the excitation monochromator slit to 2 nm.
5. Switch on (in this order) the computer, the photometric unit, the sample handling unit, and the monochromator.
6. In the stopped-flow control software, set (see note 1):
   - Excitation monochromator: 450 nm
   - Trigger: external
   - Timebase: 300s, 5000 points, logarithmic
   - Measure mode: kinetic.
7. Wash loading ports, drive syringes and flow lines:

   a) three washes with 3 ml 25 % (v/v) ethanol

   b) three washes with 3 ml H_2O

   c) three washes with 3 ml 1× Transcription Buffer.
8. Adjust the stop syringe volume to 250 μl (125 μl per drive syringe) (see note 2).
9. Prepare 1950 μl of EC mix (Table 5) without DFHBI (see notes 3-4). Incubate at 32 °C for 15 min in a thermomixer to form EC by promoter-initiated transcription with a subset of NTPs. Supplement the mix with 50 μl of 2 mM DFHBI (Table 5).

Table 5. EC mix

Volume	Reagent	Concentration	
		in the mix	in the assay
1038 µl	H_2O		
200 µl	10× Transcription Buffer	1×	1×
600 µl	Template DNA (2 µM)	600 nM	300 nM
30 µl	σ factor (200 µM)	3 µM	1.5 µM
60 µl	RNAP (100 µM)	3 µM	1.5 µM
12 µl	ApU (1 mM)	6 µM	3 µM
10 µl	ATP/GTP/CTP (2 mM each)	10 µM each	5 µM each
After 15 min incubation add:			
50 µl	DFHBI (2 mM)	50 µM	25 µM

10. Divide EC mix to two 1 ml aliquots.
11. Dilute one aliquot of EC mix with 1 ml of 1x TB buffer supplemented with proteins of interest (POI) to arrive at EC-POI(+) mix. Incubate 5 min at 32 °C.
12. Dilute the other aliquot of EC mix with 1 ml of 1x TB buffer to arrive at EC-POI(-) mix
13. Prepare 2.2 ml of NTP(+) mix and 2.2 ml of NTP(-) mix (Table 6).

Table 6. NTP(+) and NTP(-) mixes.

Volume		Reagent	Concentration	
NTP(+) mix	NTP(-) mix		in the mix	in the assay
1754.5 µl	1974.5 µl	H_2O		
220 µl	220 µl	10×Transcription Buffer	1×	1×
5.5 µl	5.5 µl	Rifampicin (10 mM)	25 µM	12.5 µM
220 µl	-	NTPs (25 mM)	250 µM	125 µM

14. Load the stopped-flow drive syringes with the desired mixes (see notes 5-6). Plan to perform four sets of stopped-flow measurements as follows (Table 7, Fig. 4).

Table 7. Four experiments required to evaluate the effect of POI on co-transcriptional RNA folding

Experiment	Left syringe	Right syringe	Purpose
a0	NTP(-) mix	EC-POI(-) mix	Background to be subtracted from #2
a1	NTP(+) mix	EC-POI(-) mix	iSpinach folding without POI

b0	NTP(-) mix	EC-POI(+) mix	Background to be subtracted from #4
b1	NTP(+) mix	EC-POI(+) mix	iSpinach folding with POI

15. Perform two injections without data acquisition to prime the stopped-flow system.
16. Perform six or more injections for each sample with data acquisition (see note 7). Save the data after each run.
17. Average 6-10 individual traces using the stopped-flow software (see notes 8-9).
18. Proceed to step 14 to perform the next set of measurements until all four sets are completed.
19. After the experiment, remove the sample syringes and wash the drive syringes and the flow lines thoroughly with milliQ water. Switch off the devices in reverse order: the monochromator, the sample handling unit, the photometric unit, the computer and, finally, the lamp. Shut off the N_2 supply and the thermostat bath.
20. Export the averaged or raw data from all experiments into the external analysis software, e.g., GraphPad Prism (GraphPad Software, La Jolla, CA, United States). Subtract the averaged background signals (experiments a0 and b0 in Table 7) from the averaged time traces of transcription experiments (experiments a1 and b1 in Table 7) to arrive at background-corrected time traces that are further analyzed as described below.

3.5 The expected outcome

For background controls (experiments a0 and b0 in Table 7), no fluorescence signal increase should be observed due to the lack of NTPs. For transcription reactions (experiments a1 and b1 in Table 7), a short (8-15 s) lag period will be observed, until transcription yields a complete DFHBI-binding iSpinach platform. Subsequently, the fluorescence signal will increase until a plateau is reached (Fig. 4). Presence or absence of RNA folding chaperones may influence the amplitude, rate of signal increase or both.

3.6 Quantification and statistical analysis

Mixing the pre-formed EC with NTPs initiates the nucleotide addition reaction by pre-formed ECs. The nucleotide addition cycle is then repeated 140-150 times to synthesize the iSpinach RNA emerging from the RNAP exit channel. The synthesized iSpinach RNA adopts a 3D structure that binds the fluorogen leading to the increase in fluorescence (Fig. 5). The fluorescence time traces feature a lag phase followed by increase in fluorescence until a plateau is reached. The lag phase corresponds to the time it takes for the fastest RNAPs to complete the synthesis of the iSpinach RNA. The duration of the lag phase, 8-15 s, is consistent with the average rate of 10-20 nt/s as expected for *E. coli* RNAP at 25-37 °C. In contrast, the increase in fluorescence occurs with the half-life of 10-30 s. The asynchronous arrival of RNAPs at the 3′ end of the iSpinach gene is likely the major component of the

observed kinetics of the fluorescence increase (Fig. 5A). Such interpretation is consistent with time courses of iSpinach RNA synthesis quantified from the RNA bands in the denaturing PAGE (Figure 4B in (Huang et al., 2020)). That said, the rate of folding of iSpinach also contributes to the kinetics of the fluorescence increase (Fig. 5A) because the RNA chaperones have been shown to modulate the rate of the fluorescence increase (Huang et al., 2020).
The background-corrected fluorescence time traces are typically adequately described by a single exponential function with a time offset (Fig. 5B):

If ($x<t_o$) $F(t)=F_o$ else $F(t)=F_o+A*(1-\exp(-k*(t-t_o)))$.

In which F(t) is the fluorescence at time t, F_o is initial fluorescence, t_o is a time offset, A is a pre-exponent parameter, and k is an exponent parameter. Fitting of the data can be performed with GraphPad Prism (GraphPad Software, La Jolla, CA, United States), Origin (Origin Labs, Northampton, MA, USA) or other similar analysis software. For statistical analysis, three or more independent experiments are performed, fluorescence time traces are fitted for each independent experiment, the inferred best-fit parameters from three or more experiments are then analyzed to determine the average values and SDs.

Noteworthy, the single exponential function unlikely reflects the underlying kinetic mechanism of the process and is used solely as an empirical function to estimate the rate (exponent) and amplitude (pre-exponent) of the fluorescence increase. RNA chaperones increase both the amplitude and the rate of the fluorescence increase (Huang et al., 2020). Accordingly, both amplitude and rates can in principle be used as measures of RNA chaperoning activities. The amplitude is arguably a more robust and easier to interpret parameter and is a preferred measure of the RNA chaperoning activities. Thus, the amplitude directly relates to the fraction of the correctly folded iSpinach (Fig. 5A). In contrast, the inferred rates are rather complex entities reflecting the broadening of the RNAP front during transcription, transcriptional pausing, and the rate of iSpinach folding.

3.7 Notes

1. The PMT voltage and V-offset should be kept constant throughout the experiment to collect data with comparable intensities.

2. It may be possible to reduce the volume settings of the stop syringe to reduce sample consumption.

3. Use a higher EC concentration in case of low signal intensities and/or low signal-to-noise ratio.

4. To prevent a noisy fluorescent signal due to light scattering by dust particles and/or precipitated proteins, all reagents should be centrifuged at > 13,000 x g and at 4 ºC for 5 minutes prior to use.

5. During sample loading, air bubbles can be trapped in the loading port and might disturb the fluorescent traces. To remove air bubbles after sample loading, rapidly push the drive syringes

up, wait until the released bubbles rise to the surface and repeat until no more air bubbles appear. Tapping of the loading syringes can detach air bubbles from the syringe walls.

6. The more precious sample should be loaded into the drive syringe that has a shorter connection to the mixing cell to limit sample consumption during priming.

7. The more curves are used for averaging, the smaller is the data scatter in the averaged curve. It is therefore advisable to measure time traces until the solutions loaded into the drive syringes are completely consumed.

8. The averaging time per data point should be less than 5 % of the reaction half-life.

9. Averaging can also be performed with external analysis software such as Microsoft Excel, GraphPad Prism (GraphPad Software, La Jolla, CA, United States), Origin (Origin Labs, Northampton, MA, USA).

4. Summary and conclusions

In this chapter we present two assays that utilize fluorogenic RNA aptamers, known as FLAPs, to monitor transcription and co-transcriptional RNA folding. The major advantage of these assays is the convenience of the real time monitoring that is characteristic for the fluorescence-based assays. The major limitation of the FLAP-based transcription assays is a relatively slow rate of the FLAP maturation that leads to the emergence of the fluorescence signal. Indeed, some RNA structures fold on the timescale of minutes and the folding kinetics is strongly affected by Mg^{2+} concentration
(Bhaskaran et al., 2012; Chadalavada et al., 2002; Chen, 2008).

In the first assay we utilize Broccoli-FLAP to measure the rate of transcription initiation. In this assay we use a multi-round setup and a large excess of RNAP over the template DNA to mitigate the slow maturation of the FLAP system. Under such conditions, the FLAP maturation steps are contained within the lag phase of a fluorescence time trace and the slope of the near linear phase reports the rate of transcription initiation. A logical evolution of the assay would be to adapt it for measuring the rate of transcription elongation. This can be principally done by utilizing two DNA templates, a template where Broccoli is placed immediately downstream of the promoter (e.g., pOP005) and a derivative template with a 2-3 kb insert between the promoter and the Broccoli-FLAP. The latter template is expected to feature a measurably longer lag phase, and the difference between the lag phases divided by the length of the insert should provide a good estimate of the transcription elongation rate.

In the second assay, we monitor the co-transcriptional folding of iSpinach-FLAP to assess the activities of RNA folding chaperones. In this assay we use a single-round setup, a pre-formed EC and a rapid mixing instrument to maximize the contribution of the FLAP maturation step to the kinetics and the amplitude of the fluorescence increase. The obvious limitation of the assay is that the folding of an unnatural RNA, iSpinach, is being monitored. A logical evolution of the assay would be to adapt it for monitoring of the folding of natural structural

RNAs such as ribosomal RNA or tRNA. To this end, embedding FLAPs at carefully selected positions within the natural structural RNAs may be the approach of choice (Okuda et al., 2017).

Finally, transcription assays described in this chapter have been developed for *E. coli* RNAP but are expected to work with RNAPs from different structural classes and different species (Alam et al., 2017; Bhadra & Ellington, 2014; Heili et al., 2018; Höfer et al., 2013; Kartje et al., 2 021; Katzmeier et al., 2019). The multi-round assay is also potentially suitable for screening and evaluating the potency of transcription inhibitors. That said, the Broccoli or iSpinach based assays may fail in the presence of compounds that strongly absorb or fluoresce in the green part of the light spectrum. Expanding the assay to employ other FLAPs that fluorescence at markedly different wavelength may provide a solution to this problem. The DIR2s-Apt-FLAP (Tan et al., 2017) is particularly promising because it fluoresces in the near-infrared range that is usually less susceptible to the interference from optically active biomolecules.

Acknowledgments

We thank Irina Artsimovitch (The Ohio State University) for providing a polycistronic plasmid for expression of *E. coli* RNA polymerase. Work in the authors' laboratories was supported by grants from the Academy of Finland (341962 to G.A.B.), the Sigrid Jusélius Foundation (to M.M-K. and G.A.B.) and the Deutsche Forschungsgemeinschaft (WA 1126/11-1 to M.C.W.).

Figure legends

Fig. 1. An overview of the multi-round Broccoli-FLAP assay for monitoring transcription initiation.

Fig. 2. Expected outcomes of the multi-round Broccoli-FLAP assay for monitoring transcription initiation. (A) Circular pOP005 template with the Broccoli gene immediately downstream the promoter assayed at four concentrations of NTPs. (B) Circular pOP004 template with the Broccoli gene ~0.6 kb downstream of the promoter assayed at four concentrations of NTPs. (C) Several concentrations of the linear pOP004 template (PCR product) assayed at 0.5 mM NTPs. Arrows denote promoters, green boxes Broccoli genes, orange boxes transcription terminators.

Fig. 3. Quantification of the multi-round Broccoli-FLAP assay for monitoring transcription initiation. (A) Schematics of the events during the pre-steady state and steady state phases of the assay. (B) The curvature of the interphase segment is likely attributed to the asynchronous arrival of pioneering RNAPs to the 3′ end of the Broccoli gene. (C) Linear fit of the fluorescence time trace (pOP005 template at 1 mM NTPs). (D) Single exponential fit of the

fluorescence time trace (pOP004 template at 1 mM NTPs). Error margins are SDs of the fit of a single experiment, larger SDs are observed when data from several independent experiments are analyzed.

Fig. 4. Workflow and expected outcome of the co-transcriptional RNA folding assay. (A) Scheme illustrating the DNA template used for the assay. (B) Setup of required solutions. a1 and b1, experiments including and excluding POI, respectively; a0 and b0, background controls including and excluding POI, respectively. (C) Multiple identical measurements (5000 data points each) are recorded. The runs are averaged, and the corresponding background signals are subtracted before further analysis.

Fig. 5. Quantification of the single-round assay for monitoring effects of POI on co-trancriptional folding of iSpinach-FLAP. (A) The asynchronous arrival of RNAPs to the 3′ end of iSpinach gene and the rate of co-trancriptional RNA folding contribute to the observed kinetics of the fluorescence increase. (B) Fluorescence time traces ± POI fit to the single exponential function (solid lines) with a time offset. Error margins are SDs of the fit of a single experiment, larger SDs are observed when data from several independent experiments are analyzed.

References

Alam, K. K., Tawiah, K. D., Lichte, M. F., Porciani, D., & Burke, D. H. (2017). A Fluorescent Split Aptamer for Visualizing RNA-RNA Assembly In Vivo. *ACS Synthetic Biology*, *6*(9), 1710–1721.

Artsimovitch, I., Chu, C., Lynch, A. S., & Landick, R. (2003). A new class of bacterial RNA polymerase inhibitor affects nucleotide addition. *Science*, *302*(5645), 650–654.

Autour, A., Westhof, E., & Ryckelynck, M. (2016). iSpinach: a fluorogenic RNA aptamer optimized for in vitro applications. *Nucleic Acids Research*, *44*(6), 2491–2500.

Bhadra, S., & Ellington, A. D. (2014). Design and application of cotranscriptional non-enzymatic RNA circuits and signal transducers. *Nucleic Acids Research*, *42*(7), e58.

Bhaskaran, H., Rodriguez-Hernandez, A., & Perona, J. J. (2012). Kinetics of tRNA folding monitored by aminoacylation. *RNA (New York)*, *18*(3), 569–580.

Cermakian, N., Ikeda, T. M., Miramontes, P., Lang, B. F., Gray, M. W., & Cedergren, R. (1997). On the evolution of the single-subunit RNA polymerases. *Journal of Molecular Evolution*, *45*(6), 671–681.

Chadalavada, D. M., Senchak, S. E., & Bevilacqua, P. C. (2002). The folding pathway of the genomic hepatitis delta virus ribozyme is dominated by slow folding of the pseudoknots. *Journal of Molecular Biology*, *317*(4), 559–575.

Chen, S.-J. (2008). RNA folding: conformational statistics, folding kinetics, and ion electrostatics. *Annual Review of Biophysics*, *37*, 197–214.

Dangkulwanich, M., Ishibashi, T., Bintu, L., & Bustamante, C. (2014). Molecular mechanisms of transcription through single-molecule experiments. *Chemical Reviews*, *114*(6), 3203–3223.

Fernandez-Millan, P., Autour, A., Ennifar, E., Westhof, E., & Ryckelynck, M. (2017). Crystal structure and fluorescence properties of the iSpinach aptamer in complex with DFHBI. *RNA (New York)*, *23*(12), 1788–1795.

Filonov, G. S., Moon, J. D., Svensen, N., & Jaffrey, S. R. (2014). Broccoli: rapid selection of an RNA mimic of green fluorescent protein by fluorescence-based selection and directed evolution. *Journal of the American Chemical Society*, *136*(46), 16299–16308.

Ganser, L. R., Kelly, M. L., Herschlag, D., & Al-Hashimi, H. M. (2019). The roles of structural dynamics in the cellular functions of RNAs. *Nature Reviews. Molecular Cell Biology*, *20*(8), 474–489.

Heikinheimo, P., Pohjanjoki, P., Helminen, A., Tasanen, M., Cooperman, B. S., Goldman, A., Baykov, A., & Lahti, R. (1996). A site-directed mutagenesis study of Saccharomyces cerevisiae pyrophosphatase. Functional conservation of the active site of soluble inorganic pyrophosphatases. *European Journal of Biochemistry*, *239*(1), 138–143.

Heili, J. M., Gomez-Garcia, J., Gaut, N. J., Cash, B. W., Aufdembrink, L. M., Heffron, B. A., Shirley, J. D., Carlson, E. E., Adamala, K. P., & Engelhart, A. E. (2018). Real-Time Visualization of *in Vitro* Transcription of a Fluorescent RNA Aptamer: An Experiment for the Upper-Division Undergraduate or First-Year Graduate Laboratory. *Journal of Chemical Education*, *95*(10), 1867–1871.

Höfer, K., Langejürgen, L. V., & Jäschke, A. (2013). Universal aptamer-based real-time monitoring of enzymatic RNA synthesis. *Journal of the American Chemical Society*, *135*(37), 13692–13694.

Huang, Y.-H., Hilal, T., Loll, B., Bürger, J., Mielke, T., Böttcher, C., Said, N., & Wahl, M. C. (2020). Structure-Based Mechanisms of a Molecular RNA Polymerase/Chaperone Machine Required for Ribosome Biosynthesis. *Molecular Cell*, *79*(6), 1024-1036.e5.

Iyer, L. M., Koonin, E. V., & Aravind, L. (2003). Evolutionary connection between the catalytic subunits of DNA-dependent RNA polymerases and eukaryotic RNA-dependent RNA polymerases and the origin of RNA polymerases. *BMC Structural Biology*, *3*, 1.

Kartje, Z. J., Janis, H. I., Mukhopadhyay, S., & Gagnon, K. T. (2021). Revisiting T7 RNA polymerase transcription in vitro with the Broccoli RNA aptamer as a simplified real-time fluorescent reporter. *The Journal of Biological Chemistry*, *296*, 100175.

Katzmeier, F., Aufinger, L., Dupin, A., Quintero, J., Lenz, M., Bauer, L., Klumpe, S., Sherpa, D., Dürr, B., Honemann, M., Styazhkin, I., Simmel, F. C., & Heymann, M. (2019). A low-cost fluorescence reader for in vitro transcription and nucleic acid detection with Cas13a. *Plos One*, *14*(12), e0220091.

Komissarova, N., Kireeva, M. L., Becker, J., Sidorenkov, I., & Kashlev, M. (2003). Engineering of elongation complexes of bacterial and yeast RNA polymerases. *Methods in Enzymology*, *371*, 233–251.

Krupp, F., Said, N., Huang, Y.-H., Loll, B., Bürger, J., Mielke, T., Spahn, C. M. T., & Wahl, M. C. (2019). Structural Basis for the Action of an All-Purpose Transcription Anti-termination Factor. *Molecular Cell*, *74*(1), 143-157.e5.

Leamy, K. A., Assmann, S. M., Mathews, D. H., & Bevilacqua, P. C. (2016). Bridging the gap between in vitro and in vivo RNA folding. *Quarterly Reviews of Biophysics*, *49*, e10.

Neubacher, S., & Hennig, S. (2019). RNA Structure and Cellular Applications of Fluorescent Light-Up Aptamers. *Angewandte Chemie (International Ed. in English)*, *58*(5), 1266–1279.

Okuda, M., Fourmy, D., & Yoshizawa, S. (2017). Use of Baby Spinach and Broccoli for imaging of structured cellular RNAs. *Nucleic Acids Research*, *45*(3), 1404–1415.

Prajapati, R. K., Rosenqvist, P., Palmu, K., Mäkinen, J. J., Malinen, A. M., Virta, P., Metsä-Ketelä, M., & Belogurov, G. A. (2019). Oxazinomycin arrests RNA polymerase at the polythymidine sequences. *Nucleic Acids Research*, *47*(19), 10296–10312.

Said, N., & Wahl, M. C. (2021). Transcription complexes as RNA chaperones. *Transcription*, *12*(4), 126–155.

Schärfen, L., & Neugebauer, K. M. (2021). Transcription regulation through nascent RNA folding. *Journal of Molecular Biology*, *433*(14), 166975.

Svetlov, V., & Artsimovitch, I. (2015). Purification of bacterial RNA polymerase: tools and protocols. *Methods in Molecular Biology*, *1276*, 13–29.

Tan, X., Constantin, T. P., Sloane, K. L., Waggoner, A. S., Bruchez, M. P., & Armitage, B. A. (2017). Fluoromodules consisting of a promiscuous RNA aptamer and red or blue fluorogenic

cyanine dyes: selection, characterization, and bioimaging. *Journal of the American Chemical Society*, *139*(26), 9001–9009.

Werner, F., & Grohmann, D. (2011). Evolution of multisubunit RNA polymerases in the three domains of life. *Nature Reviews. Microbiology*, *9*(2), 85–98.

Yu, A. M., Gasper, P. M., Cheng, L., Lai, L. B., Kaur, S., Gopalan, V., Chen, A. A., & Lucks, J. B. (2021). Computationally reconstructing cotranscriptional RNA folding from experimental data reveals rearrangement of non-native folding intermediates. *Molecular Cell*, *81*(4), 870-883.e10.

Zhang, J., & Landick, R. (2016). A Two-Way Street: Regulatory Interplay between RNA Polymerase and Nascent RNA Structure. *Trends in Biochemical Sciences*, *41*(4), 293–310.

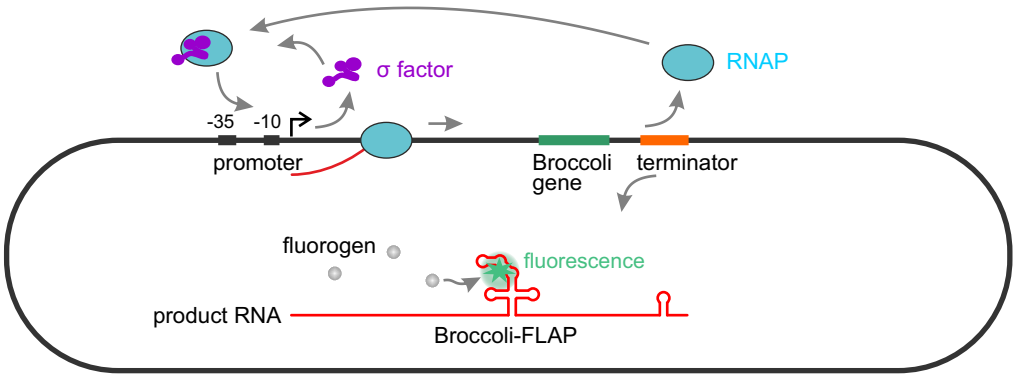

Fig. 1. An overview of the multi-round Broccoli-FLAP assay for monitoring transcription initiation.

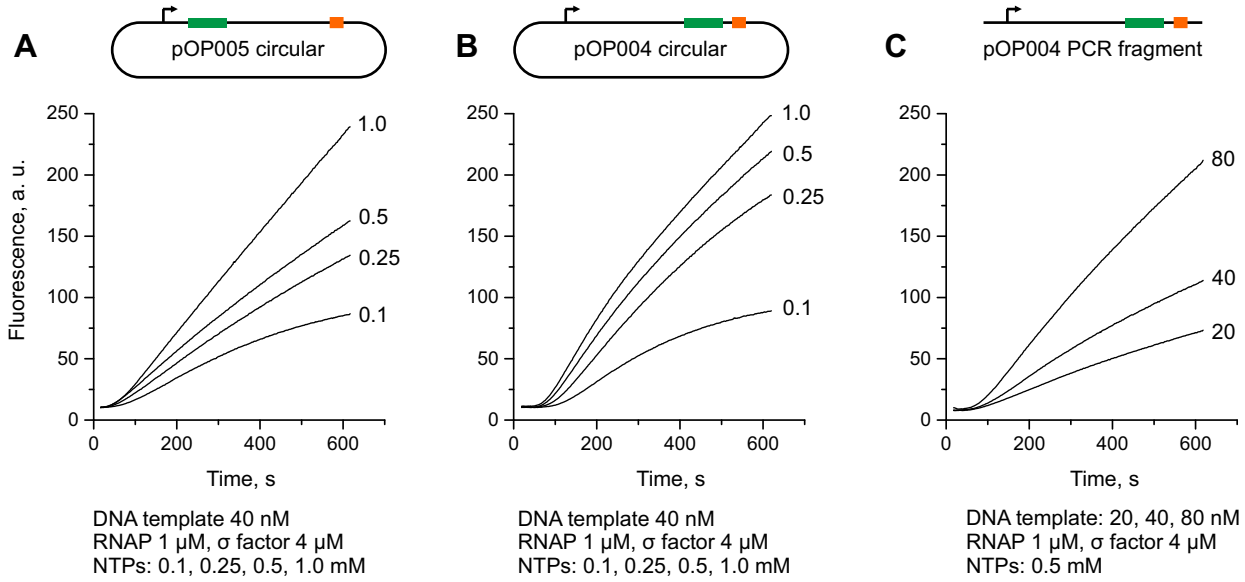

Fig. 2. Expected outcomes of the multi-round Broccoli-FLAP assay for monitoring transcription initiation. (A) Circular pOP005 template with the Broccoli gene immediately downstream the promoter assayed at four concentrations of NTPs. (B) Circular pOP004 template with the Broccoli gene ~0.6 kb downstream of the promoter assayed at four concentrations of NTPs. (C) Several concentrations of the linear pOP004 template (PCR product) assayed at 0.5 mM NTPs. Arrows denote promoters, green boxes Broccoli genes, orange boxes transcription terminators.

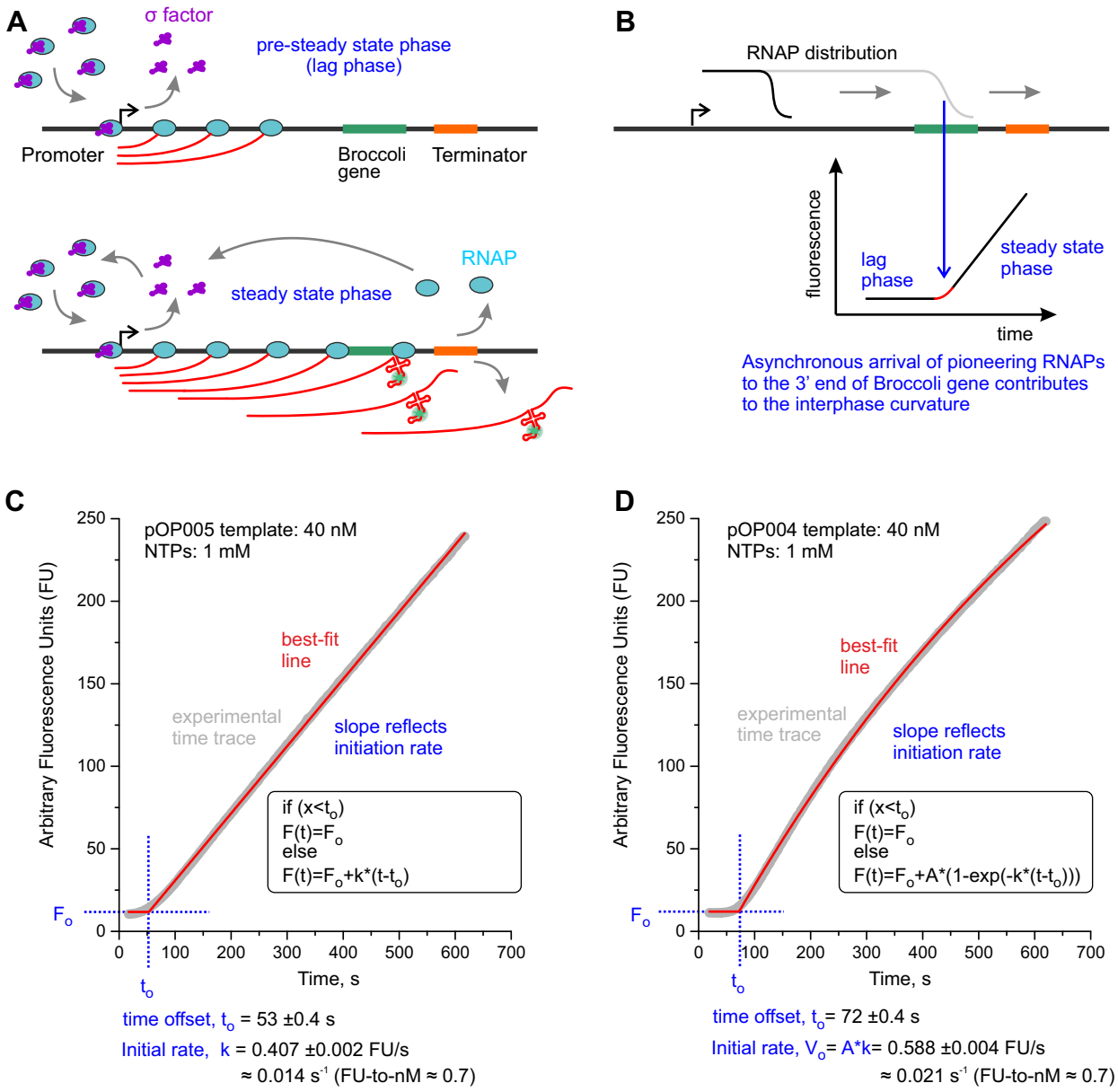

Fig. 3. Quantification of the multi-round Broccoli-FLAP assay for monitoring transcription initiation. (A) Schematics of the events during the pre-steady state and steady state phases of the assay. (B) The curvature of the interphase segment is likely attributed to the asynchronous arrival of pioneering RNAPs to the 3' end of the Broccoli gene. (C) Linear fit of the fluorescence time trace (pOP005 template at 1 mM NTPs). (D) Single exponential fit of the fluorescence time trace (pOP004 template at 1 mM NTPs). Error margins are SDs of the fit of a single experiment, larger SDs are observed when data from several independent experiments are analyzed.

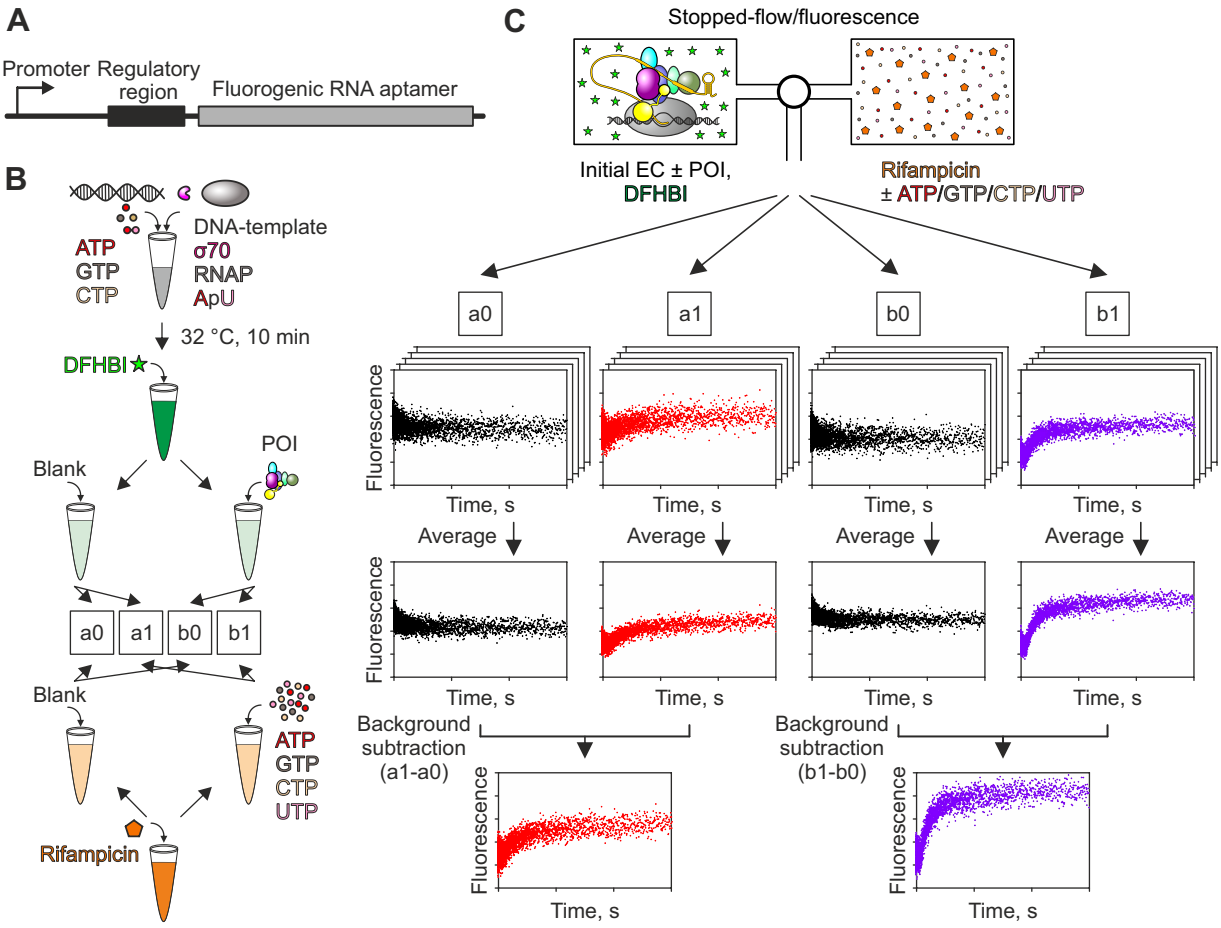

Fig. 4. Workflow and expected outcome of the co-transcriptional RNA folding assay. (A) Scheme illustrating the DNA template used for the assay. (B) Setup of required solutions. a1 and b1, experiments including and excluding POI, respectively; a0 and b0, background controls including and excluding POI, respectively. (C) Multiple identical measurements (5000 data points each) are recorded. The runs are averaged, and the corresponding background signals are subtracted before further analysis.

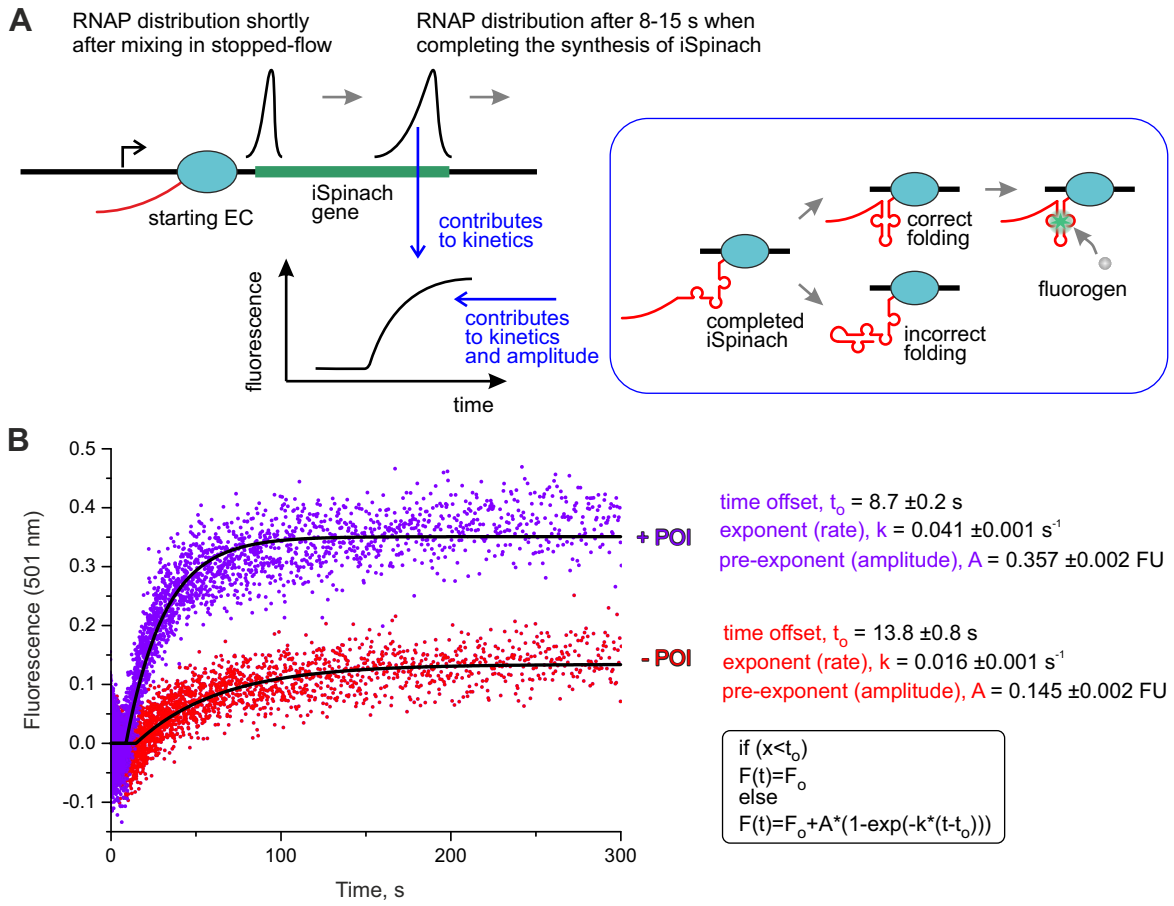

Fig. 5. Quantification of the single-round assay for monitoring effects of POI on co-trancriptional folding of iSpinach-FLAP. (A) The asynchronous arrival of RNAPs to the 3' end of iSpinach gene and the rate of co-trancriptional RNA folding contribute to the observed kinetics of the fluorescence increase. (B) Fluorescence time traces ± POI fit to the single exponential function (solid lines) with a time offset. Error margins are SDs of the fit of a single experiment, larger SDs are observed when data from several independent experiments are analyzed.